

AD-A060 762

MARTIN MARIETTA LABS BALTIMORE MD  
COMBUSTION PROPERTIES OF HIGH-DENSITY FUELS. (U)  
MAY 77 M T MCCALL, J M BRUPBACHER

F/G 21/4

UNCLASSIFIED

MML-TR-77-34C

N00019-76-C-0683

NL

| OF |  
AD  
A060 762

END  
DATE  
FILED  
1-79  
DDC

AD A060762

DDC FILE COPY

MARTIN MARIETTA

# Martin Marietta Laboratories

LEVEL II  
APPROVED FOR PUBLIC RELEASE:  
DISTRIBUTION UNLIMITED

MMI TR 77-34c

1  
NW

COMBUSTION PROPERTIES OF HIGH-DENSITY FUELS

Quarterly Report No. 2

Prepared by:

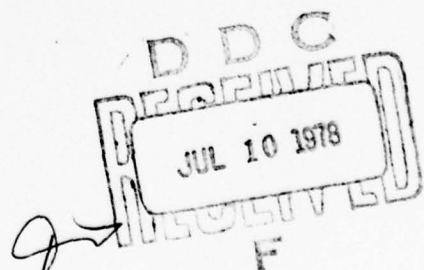
M. Thomas McCall and John M. Brupbacher

Prepared for:

Department of the Navy  
Naval Air Systems Command  
Washington, D.C. 20361

Under Contract No.: N00019-76-C-0683

May 1977



07 06 06 2

(6)

## COMBUSTION PROPERTIES OF HIGH-DENSITY FUELS

(9)

Quarterly Report No. 2, 1 Feb - 30 Apr 77

Period Covered: February 1, 1977 through April 30, 1977

(10)

M. Thomas McCall and John M. Brupbacher  
MARTIN MARIETTA CORPORATION  
Martin Marietta Laboratories  
1450 South Rolling Road  
Baltimore, Maryland 21227

(12) 28P.

(14) MML-TR-77-34c

(11)

May 1977

Prepared for  
DEPARTMENT OF THE NAVY  
Naval Air Systems Command  
Washington, D.C. 20361

Under Contract N0019-76-C-0683

(15)

ACCESSION FOR	White Section
NTIS	White Section
PPC	B-B Section <input type="checkbox"/>
ANNOUNCED	<input checked="" type="checkbox"/>
TESTIFICATION	
BY	
DISTINGUISHING FEATURES	
A	

78 07 06 062  
407 998

SLV

### Introduction

The proposed fuel, RJ-5, is a blend of several fused ring hydrocarbons of low carbon/hydrogen ratio. This property imparts high density and high volumetric heat of combustion to the fuel, features which make it a promising candidate for volume-limited applications such as the ASALM program. Unfortunately, the need for improvements in several of its physical properties, such as freezing point and viscosity, as well as production-related difficulties, have necessitated modification of the fuel's isomer ratio and the use of additives.

It is well established that small quantities of additives can have major effects on combustion parameters such as flame velocity<sup>(1)</sup>, first and second ignition delays<sup>(2)</sup>, and hot-wire ignition temperatures<sup>(3)</sup>. Many of these effects are difficult to predict a priori and to explain a posteriori. For this reason, considerable interest has been generated in the development of new and innovative techniques to monitor the effect of variation in fuel composition and to obtain a better understanding of fuel combustion kinetics by using additives to tailor fuel performance to engine needs.

One promising tool for combustion research is the chemical shock tube. With this method, fuel-air mixtures can be rapidly heated to a preselected temperature and pressure, and their combustion can be studied free from the complicating temperature, pressure, and density gradients associated with flame studies.

Two previous shock tube studies on the combustion kinetics of RJ-5 have been carried out by Shell<sup>(4)</sup>, and Martin Marietta Laboratories (MML)<sup>(5)</sup> to measure ignition delays,  $\tau$ . The goals of these preliminary

studies were to: (1) investigate the effect of reaction conditions on  $\tau$ , and (2) determine the influence of viscosity-reducing additives. While extensive data on the variation of  $\tau$  were obtained with the experimental techniques employed, it is not clear how these data would correlate with engine test firing results because  $\tau$  is merely an indicator of the onset of combustion and is not directly related to combustion duration or efficiency.

Because of the uncertainties associated with ignition-delay measurements, a more extensive study was carried out at MML to establish procedures for monitoring the entire combustion profile for RJ-5 vapor-air mixtures rather than just ignition<sup>(6)</sup>. In this study, the infrared emissions emanating from a hot shock-initiated combustion zone were filtered to yield CO<sub>2</sub> and H<sub>2</sub>O time profiles. From these data, the effect of variation in the reaction temperature, pressure, and fuel/air ratio on the combustion rate and duration were obtained.

It was recognized, however, that combustion in real systems is heterogeneous, i. e., ignition of fuel vapor occurs first, followed by the much slower burning of a fine mist of liquid droplets in the hot combustion zone. This aspect of the combustion problem is more significant for RJ-5 than for JP-4 or 7 because RJ-5's higher viscosity leads to much larger droplets due to air blast shearing in rocket engines<sup>(7)</sup>.

The present work has been undertaken to study the heterogeneous combustion of RJ-5 air mist. To study this complex but technically more realistic situation, we have added an ultrasonic nebulizer to the downstream end of a shock tube (Fig. 1). With this device, a fine mist of controlled particle size and concentration is generated near the shock

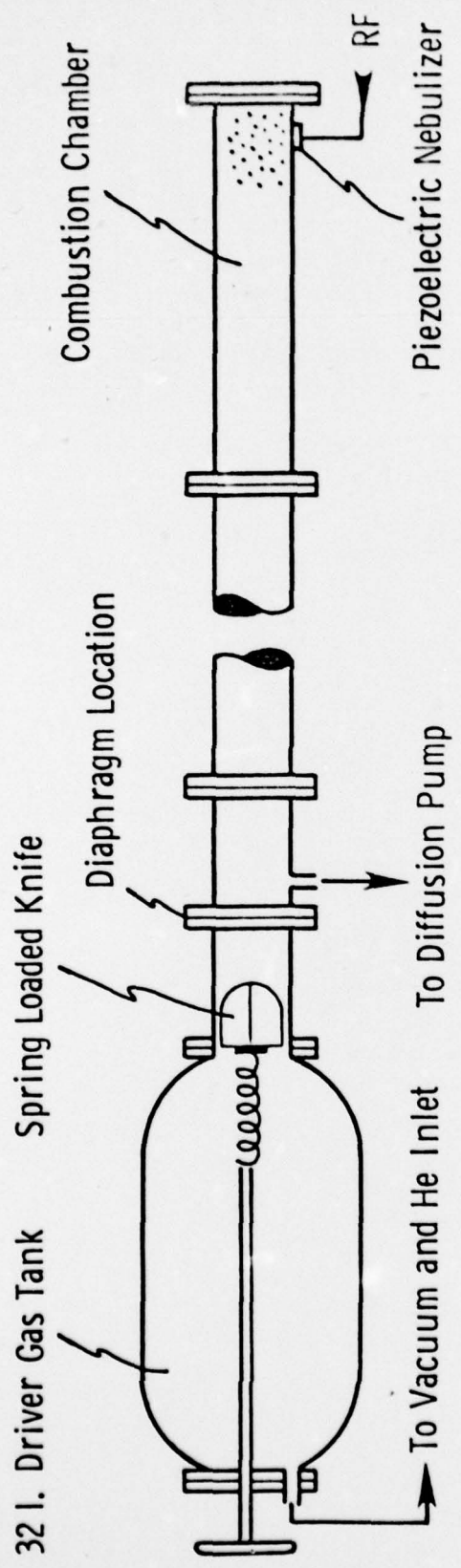


Figure 1. General schematic of nebulizer-coupled shock tube.

tube end wall. A shock wave is initiated through air, compressing and heating the mist and causing combustion of the atomized fuel. The construction details of the nebulizer-coupled shock tube system have already been discussed<sup>(8)</sup>.

The present report will be concerned with the formation, stability, and characterization of the precombustion shock-induced RJ-5 air mist.

#### Shock Wave Production

Since combustion in heterogeneous systems must be preceded by vaporization, it is inherently slower than simple vapor phase combustion. This difference would probably lead to combustion times that would exceed the reflected shock wave duration of the existing MML system.

To a first approximation, the useable duration of the reflected shock zone is proportional to the shock tube length. However, wall drag (in small diameter tubes) and inadequate diaphragm openings are important parameters in causing reflected shock decay. It was felt that these deficiencies could not be overcome with the existing shock tube. Consequently, a new tube has been constructed to eliminate these two difficulties.

To ensure uniform and rapid diaphragm rupture, a spring-loaded, double-bladed knife has been installed into the driver sections. Diaphragm rupture is initiated by release of the cocked knife which accelerates downstream and cuts the diaphragm in a quadrant petaling pattern. The knife is rapidly retracted from the foil region by spring tension, producing an unhindered path for driver gas expansion, and hence, a longer lifetime for the reflected zone. Aluminum diaphragms retain their post-shock configuration and, readily exhibit the quadrant pattern (Fig. 2).

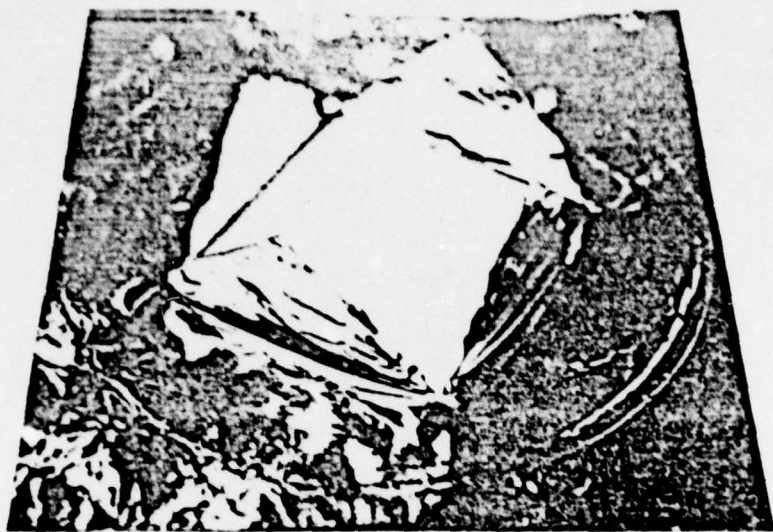


Figure 2. (a) Photograph of ruptured aluminum diaphragm showing quadrant petaling pattern.

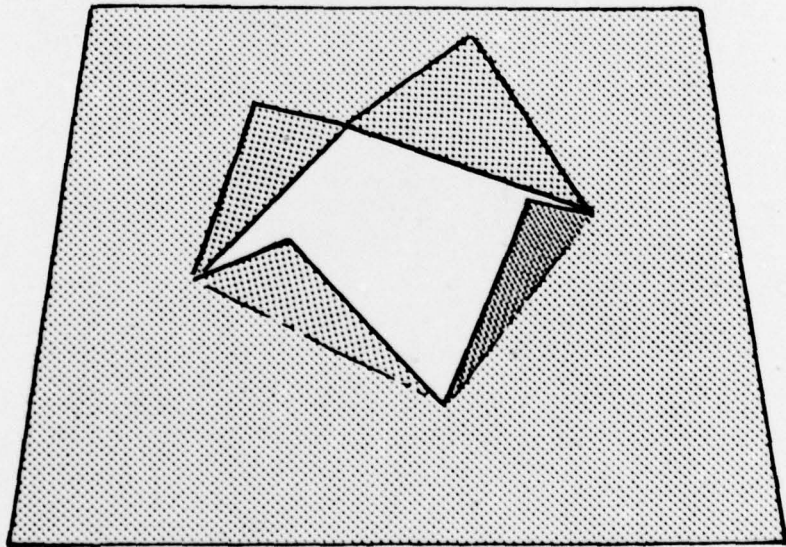


Figure 2. (b) Artist conception of above.

To minimize the effect of wall drag, 1.75 in. i.d. square polished aluminum pipe was used for the shock tube construction instead of the 1 in. i.d. circular tubing previously employed. This corresponds to a fourfold increase in shock tube cross-sectional area, which should significantly reduce drag effects. Furthermore, care was taken to ensure that shock tube attachments, e.g., windows, valves, pressure transducers, etc., were flush-mounted to limit turbulent effects.

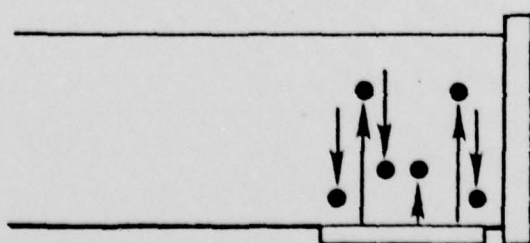
Figure 3 shows clearly that the reflected shock zone is stable beyond  $1500 \mu$  sec. As will be demonstrated later, this time interval should be ample for vaporization and combustion of the fuel mist.

#### Aerosol Characterization

The coupling of an ultrasonic nebulizer and shock tube has not previously been attempted. For this reason, procedures for mist characterization in shock tubes have not been fully established. Hence, the factors affecting aerosol properties are discussed in some detail below.

##### 1) Particle Concentration

Upon initiation of nebulization in the preshocked combustion zone, a fine air mist will be formed. However, droplet settling will begin immediately. This process is depicted in the figure shown below.



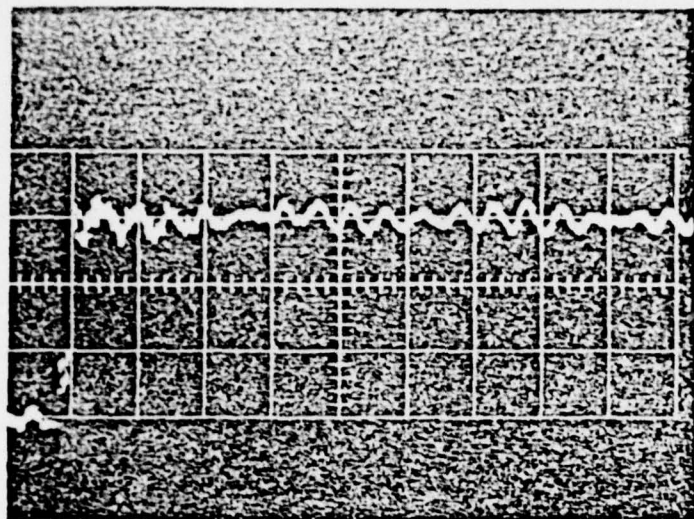


Figure 3. (a) Polaroid record of pressure profile during shock experiment at  $2000^{\circ}\text{K}$ ; sweep speed equals  $200 \mu\text{sec.}/\text{cm.}$

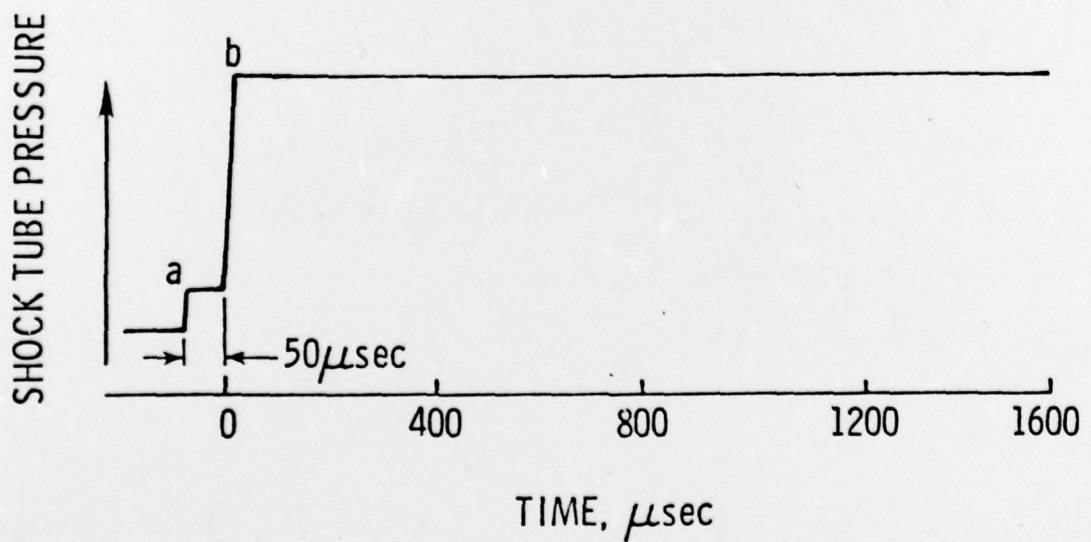


Figure 3. (b) Line drawing of above experiment  
 a) Incident shock arrival at observation station;  
 b) Reflected shock arrival at same station.

A steady state situation between particle formation and settling will rapidly be achieved; thus, the mist concentration will be independent of time. This is represented mathematically by the expression

$$\Delta(\text{droplets})/\Delta\text{time} = 0 = k_N - k_S \quad (\text{droplets})$$

where  $k_N$  and  $k_S$  are the nebulization and settling rate constants, respectively. Thus, the steady droplet concentration, (droplets), is given by

$$(\text{droplets}) = \frac{k_N}{k_S} .$$

The value of  $k_N$  can be obtained from the time required to nebulize a known quantity of fuel under a flowing condition where the droplets cannot return to the transducer surface. The settling rate constant can be calculated as discussed below. Thus, both factors affecting the steady state particle concentration can be readily obtained.

The settling velocity of spherical particles in a stagnant air mass is given by the "tranquil settling expression" (9).

$$C = \frac{g d^2 (\rho_p - \rho_m)}{18 \eta}$$

where  $d$  is the droplet diameter,  $\eta$  is the viscosity of the medium, and  $\rho_p$  and  $\rho_m$  are the densities of the particles and settling medium, respectively. For RJ-5 droplets in air,  $\rho_{\text{air}} \ll \rho_{\text{RJ-5}}$  and, hence, can be neglected. Also, the viscosity of air is essentially independent of pressure over the region of interest. The calculated settling rates of the droplet sizes of interest to the present study, those of diameter 0.5 - 50  $\mu$ , are given in Table I.

Of significance here is the fact that the particle settling time, indicated  $1/C$ , is a strong function of particle diameter. This has two

TABLE I.  
Settling Rates of RJ-5 Droplets in Air

dp ( $\mu$ )	C (cm/sec.)	1/C (sec./cm)
0.5	$3.27 \times 10^{-3}$	306
1.0	$1.31 \times 10^{-2}$	76.5
5	$3.27 \times 10^{-1}$	3.06
10	$1.31 \times 10^0$	0.765
50	$3.27 \times 10^1$	0.0306

g = 980 cm/sec.,  $\eta_{air}^{20^{\circ}D} = 1.8 \times 10^{-4}$  poise,  $\rho_{RJ-5} = 1.08 \text{ g/cm}^3$

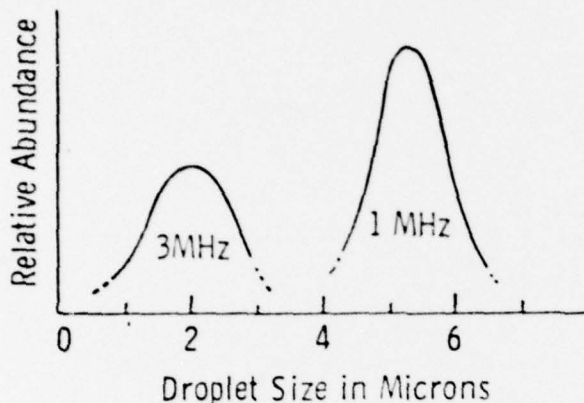
implications with regard to mist structure:

- It will be necessary to vary the irradiation power to maintain the same droplet concentration as the mean droplet diameter is varied via the irradiation frequency; and
- The steady-state particle distribution of the mist will differ somewhat from that of the droplets as they leave the transducer surface. Fortunately, ultrasonic nebulizers have fairly narrow distribution curves. Hence, this difference should not pose any serious problems to mist characterization.

2) Particle Size Distribution

In addition to the ease with which it could be coupled to the shock tube, an important reason for the choice of the ultrasonic nebulizer for producing the fuel aerosol was its ability to vary the mean particle size.

Furthermore, as mentioned previously, the distribution is relatively narrow. This is exemplified in the data given by Denton<sup>(10)</sup> (below).



However, the theory of ultrasonic nebulizers has not been adequately developed to account for changes in liquid physical properties, such as viscosity, surface tension, etc. Consequently, it will be necessary to experimentally determine the droplet size distribution curve for RJ-5 as a function of the irradiation frequency. Of the various methods available, the approach taken by Kousaka<sup>(9)</sup> seems ideally suited for nebulizer characterization. In this method, particle size distribution is determined by the time and number of particles settling through the depth of focus of an ultramicroscope. This method has been successfully employed to characterize water aerosols in the range of 0.5 to 10  $\mu$ . The equipment necessary to carry out this procedure is presently available at MML.

### 3) Particle Vaporization

Prior to shock arrival in the mist region, the RJ-5 liquid-vapor

equilibrium will already be established. Consequently, mass loss through vaporization will not be a significant problem in the preshock mist. However, vaporization will begin immediately upon shock heating. The total time required to vaporize the droplets in a stagnant, non-combustion atmosphere, e.g., a shock-heated nitrogen, rather than air-mist, can be readily calculated from the relationship (refer to Appendix I)

$$\tau_v = \rho H_v r_o^2 / (2\lambda [T_m - T_d])$$

where  $H_v$  is the heat of vaporization,  $r_o$  the initial drop radius,  $\lambda$  is the thermal conductivity of the atmosphere, and  $T_m$  and  $T_d$  are the air and drop temperatures, respectively. For instance, a 50  $\mu$  (dia.) drop of RJ-5, initially at 300 $^{\circ}$ K and shock heated to 1273 $^{\circ}$ K (1000 $^{\circ}$ C), will completely vaporize in about 1400  $\mu$  sec., which is about the lifetime of the reflected shock zone (refer to Fig. 3). However, when surrounded by flame in a combustion environment, the vaporization time will be substantially less. Therefore, it is unlikely that combustion of 50  $\mu$  RJ-5 droplets would be incomplete in the observation time available.

#### 4) Axial Stability

Upon arrival of the incident shock wave in the mist region, the aerosol particles will suddenly come under the influence of a frictional force or drag, which, given time, will accelerate them to supersonic shock speed. Fortunately, however, the accelerating force is instantly neutralized when the particles collide with the stagnant reflected shock zone. Although the time between the incident and reflected shock arrival,  $t$ , is short -- about 50  $\mu$  sec. (refer to Fig. 3), the particles will have a finite velocity in the direction of the end plate when they

enter the reflected zone. Similarly, they will then decelerate due to frictional drag with the stationary reflected shock gasses. Since it is important that the burning RJ-5 mist remain in the viewing region (located about 1 cm from the end plate) and not be swept into it during the observation time, an analysis of the mist axial drift is presented below.

According to Stokes, a spherical particle moving in a stationary gas stream, or conversely, a gas stream flowing over a stationary particle, will exert a frictional force on the particle described by the relationships<sup>(11)</sup>

$$\text{Force} = 6 \pi \eta r v = -m \frac{dv}{dt}$$

where  $r$  and  $m$  are the particle radius and mass, respectively, and  $v$  is the particle velocity relative to the gas. This relationship leads to the expression for the particle speed,  $s$ , relative to the side viewing port (Appendix II).

$$s = a \left[ 1 - e^{-\frac{4.5 \eta t}{r^2 \rho}} \right]$$

where  $\rho$  is the droplet density, and "a" is the incident shock velocity. The velocity,  $s$ , of a 50  $\mu$  dia. RJ-5 droplet exposed to a Mach 2 incident shock wave would be 1380 cm/sec. after 50  $\mu$  sec. Thus, during this 50  $\mu$  sec., it would have moved only 0.35 mm from its original preshock position. Furthermore, the reflected shock gas viscosity, and hence its decelerating force, would be substantially higher than in the incident zone due to the higher temperature. Consequently, droplets of approximately this size should remain in the observation region during combustion.

### SYMBOLS

$k_N$	nebulization rate
$k_S$	droplet settling rate
$d$	droplet diameter
$\eta$	viscosity of gaseous medium
$\rho$	droplet density
$\rho_m$	density of gaseous medium
$c$	settling velocity
$\tau_v$	vaporization time
$H_v$	heat of vaporization
$\lambda$	thermal conductivity of medium
$T_m$	temperature of medium
$T_d$	temperature of drop
$t$	incident shock time at observation station
$v$	relative particle velocity
$r$	particle radius
$m$	particle mass
$s$	axial particle velocity

#### REFERENCES

1. H. G. Wagner, "Studies of Inhibitors as Anticatalytic Extinction Agents (Preliminary Report)", Research Contract No. 3155 (1955).
2. B. Lewis and G. von Elbe, Combustion, Flames and Explosions of Gases, 2nd Ed., Chapter IV, Academic Press, New York (1961).
3. M. E. Morrison and K. Scheller, Combust. Flame, 18, 3 (1972).
4. A. D. Nixon et al., Shell Oil Company, Final Report Part II, AFAPL-TR-67-114.
5. M. McCarty, Jr., J. N. Maycock, and D. Skean, presented at Western States Section, The Combustion Institute, Monterey, California, October 30-31, 1972.
6. J. M. Brupbacher, M. T. McCall, and M. McCarty, "Combustion of High Density Fuels", MML Final Report, Contract No. N00019-76-C-0200, November 1976.
7. Private communication, Ed Cobb, Martin Marietta Corporation.
8. M. T. McCall and J. M. Brupbacher, "Combustion Properties of High Density Fuels", MML Quarterly Report, Contract No. N00019-76-C-0683, January 1977.
9. T. Yoshida, Y. Kousaka, and K. Okugama, Ind. and Eng. Chem. Fund., 14, 47 (1975).
10. M. B. Denton, D. B. Swartz, Rev. Sci. Instrum., 45, 81, 1974.
11. R. B. Bird, W. E. Steward, and E. N. Lightfoot, "Transport Phenomena", John Wiley and Sons, New York (1960).

## APPENDIX I.

The rate of heat transfer to a spherical drop of RJ-5 from the surrounding atmosphere,  $dg/dt$ , is<sup>(12)</sup>

$$dg/dt = 4 \pi r \lambda (T_m - T_d)$$

where  $\lambda$  is the thermal conductivity of the atmosphere. It is assumed that all the heat transferred is used to vaporize RJ-5 at constant temperature  $T_d$ , then

$$dg/dt = -H_v dm/dt = 4\pi \rho r^2 H_v dr/dt, \text{ where}$$

where  $H_v$  is the heat of vaporization per unit weight, and  $\rho$  is the density of RJ-5. Combining these two equations leads to

$$dr/dt = -\lambda (T_a - T_d) / (\rho r H_v)$$

which, upon integration, leads to an expression for the total vaporization time,

$$\tau_v = \rho H_v r_o^2 / [2\lambda(T_a - T_d)].$$